Chapter 2

Fundamentals

In this first chapter, the basic structural properties of microcrystalline silicon as well as their consequences for the density of states are discussed. As the electronic density of states (DOS) is mainly determined by the disorder of the system, the nature of band-tail states and deep defects are discussed. In the third section of this chapter the transport properties are outlined with respect to the DOS.

2.1 Structural Properties of Microcrystalline Silicon

Microcrystalline silicon (μc-Si:H) as referred to in the literature describes a wide range of silicon material rather than a well defined structure. In fact, μc-Si:H is a general term for a silicon composition containing varying amounts of crystalline grains, amorphous phase, and voids. These phases are separated from each other by a disordered silicon tissue or grain boundaries additionally complicating the structure. To obtain a picture of the structure, a number of characterization methods, e.g. transmission electron microscopy (TEM), X-ray diffraction (XRD), and Raman spectroscopy, have been applied in the past [10, 50, 51]. A schematic picture of the structure derived from these works is shown in Fig. 2.1. The figure shows a wide range of material structures ranging from highly crystalline, left hand side, to predominantly amorphous growth on the right hand side. The particular structure of the μc-Si:H strongly depends on the deposition conditions. The transition in growth can be achieved by varying a number of different deposition parameter, as has been demonstrated by Roschek, [53], Vetterl [12] for plasma enhanced chemical vapor deposition (PECVD), and by Klein [13] for material prepared by hot-wire chemical vapor deposition (HWCVD). In particular the silane concentration is very useful to control the crystallinity of the μc-Si:H material. However, the structure not only depends on the deposition conditions, but also on the substrate used. In particular for material deposited at the transition

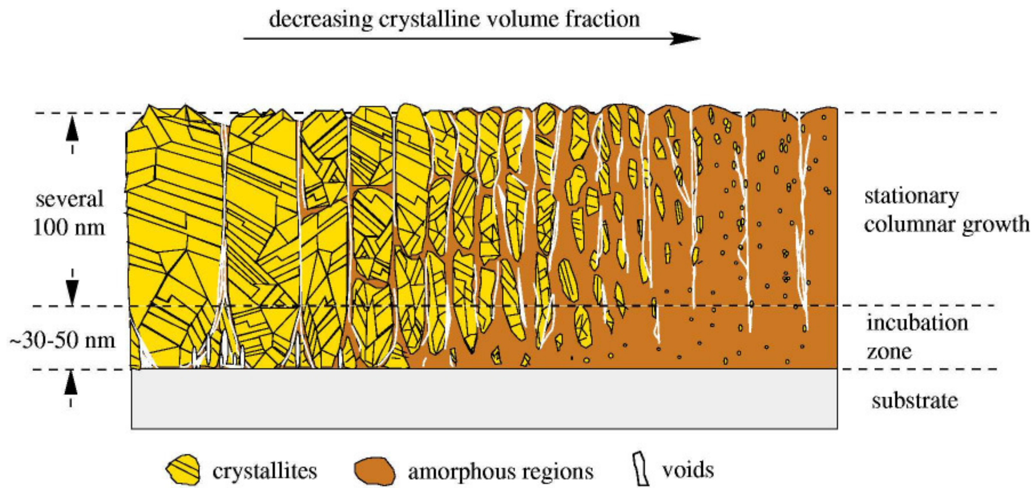

Figure 2.1: *Schematic picture of structure features found in μc-Si:H. From left to right the film composition changes from highly crystalline to amorphous. The picture was taken from Houben [52]*

between μc-Si:H and a-Si:H growth, the structure varies significantly depending on the substrate. While for a fixed set of process parameters the material deposited on aluminum foil results in crystalline growth, fully amorphous structure can be observed for the one deposited on glass [54, 55, 50]. The substrate dependence is of particular importance and has to be kept in mind if one wants to compare results obtained from different measurement techniques, since different substrates, e.g. glass or aluminum, are required for different methods.

Typical for all structure modifications is the occurrence of an incubation zone. The particular thickness and composition of this region strongly depends on the deposition condition and the substrate used. In the highly crystalline regime, crystallization starts from nucleation centers close to the substrate-film interface. With increasing film thickness the diameter of the columnar structures increases resulting in the typically observed conical shape. In the highly crystalline regime the columnar clusters of coherent regions have a diameter of up to 200 nm and extend over the whole film thickness. However, the structure inside the columns is not monocrystalline. In fact it consists of coherent regions with a diameter of 4 – 20 nm that are separated from each other by stacking faults and twin boundaries [10, 50, 56, 57, 58].

The columns themselves are separated from each other by crack-like voids and disordered material. In fact, studies using transmission electron microscopy (TEM) [50, 10], infrared spectroscopy (IR) [11, 59], and hydrogen effusion [60] have shown that highly crystalline material often exhibits a pronounced porosity.

Studies have also shown that these voids may extend from the surface deep into the film and allow for in-diffusion of atmospheric gases along the column boundaries [20, 22].

An increasing amorphous phase content leads to a reduction of the column diameter, while an extended disordered phase is incorporated in the increasing incubation layer and at the column boundaries. Concerning the porosity there is some not yet understood discrepancy between results obtained from TEM and IR. While TEM shows cracks and voids, there is no indication of oxygen in-diffusion or low temperature hydrogen effusion in such material, suggesting a rather compact structure. At the site of transition between crystalline and amorphous growth, the material structure changes significantly. The columns no longer extend throughout the entire film thickness. In fact, the crystalline regions are frequently interrupted and embedded in an amorphous matrix. The size of the crystalline domains decreases as the size of the coherent regions forming them. Finally only amorphous growth is obtained and no crystalline contribution can be found in the material. However, the electronic properties of the amorphous phase found in this kind of material differs from standard a-Si:H and is therefore often referred to as ”protocrystalline”, ”polymorphous” or ”edge material” [61, 62, 63].

2.2 Electronic Density of States

The structural properties of μc-Si:H, in particular the disorder, lead to some phenomena in the electronic density of states (DOS) that cannot be found in the crystalline counterpart. The lack of translational symmetry leads to some major consequences for the electronic properties of the material. However, as the electronic structure is mostly determined by the short range order, the overall electronic properties are very similar compared to the equivalent crystal. But, due to the lack of long range order, the abrupt band edges found in the crystal are replaced by a broadened tail of states extending into the forbidden gap. On the other hand, the deviation from the ideal network structure also results in electronic states deep within the gap (dangling bonds). As microcrystalline silicon is a phase mixture of crystalline and disordered regions separated by grain boundaries and voids, the particular band structure dependents on the particular spatial position within the material, and an overall DOS-diagram can not be drawn easily.

In the following section a brief description of the main features of the DOS is given. On the basis of the simplified picture for the DOS in a-Si:H, shown in Fig. 2.2, band-tail and defect states are discussed and adopted for a description of the DOS of μc-Si:H. Note, while the schematic DOS for a-Si:H shown in Fig. 2.2 is sufficient to describe a number of experimental results including electron spin

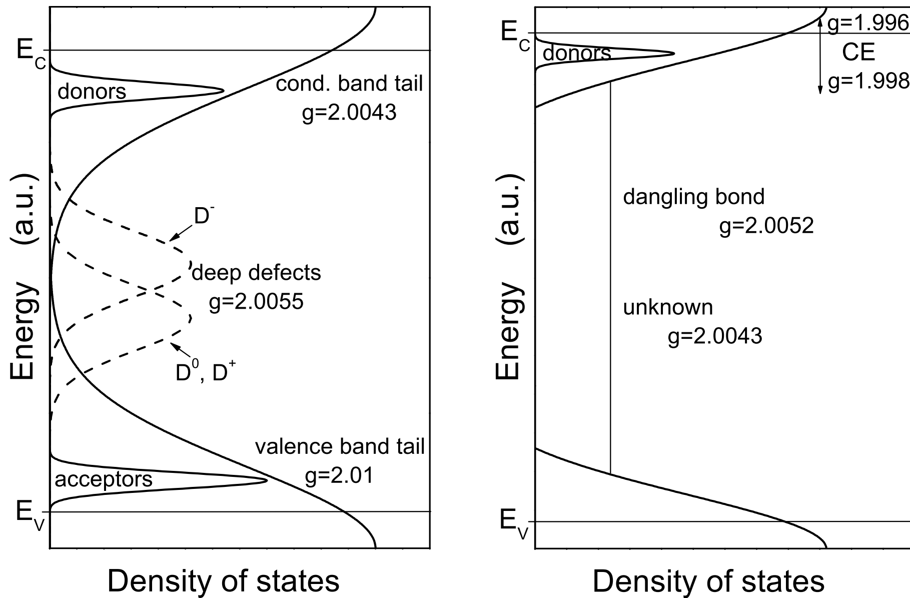

Figure 2.2: *Schematic density of states of amorphous (left) [65] and microcrystalline (right) silicon [39].*

resonance (ESR) very well, there are other models for the distribution of defects, e.g. the so-called defect-pool model (see e.g. [64] for a review), which however will not be treated here.

2.2.1 Band-Tail States

One consequence of a missing long range order is the existence of band-tail states. Local fluctuations in the interatomic distances and the bonding angles result in spatial fluctuations of the band edges. This leads to regions within the band, where charge carriers can be trapped. The existence of localized states in disordered material was first predicted by Anderson [66], and it has been shown by Mott that any random potential introduces localized states in the tails of the band [67, 68]. The resulting DOS is schematically shown in Fig. 2.2, where the usually sharp band edges are replaced by a broad tail extending deep into the bandgap. Within the band-tail localized and extended states are separated by mobility edges at energies E_C or E_V, respectively. The mobility edge derives its name from the fact that at zero temperature only charge carriers above E_C (for E_V below) are mobile and contribute to transport [68]. While these ideas have been developed and experimentally proven mainly for amorphous material, it has been shown by Werner et al. [69, 70, 71] that for poly-crystalline silicon, the spatial distribution of defects at grain boundaries also leads to potential fluctuations, resulting in band-

tail states.

As grain boundaries and amorphous phase content are an inherent structure feature of μc-Si:H, it is most likely, that localized band-tail states might also exist is this material class. Evidence for the existence of band-tail states comes from e.g. electron spin resonance [39, 72], electrical transport measurements [73], photo deflection spectroscopy [44], and photo luminescence measurements [74, 75]. From transient photocurrent measurements on a-Si:H material one can deduce that the tail falls exponentially towards the mid-gap (for a review see e.g. [76]). The same shape was also found in poly-crystalline silicon [69, 70] and has lately been adopted to μc-Si:H [77, 75, 73]. Though the exact underlying reasons are unclear, theoretical works confirm the existence of exponential tails [78, 79, 80, 81, 82]. The particular width of the band-tail depends on the bonding character of the states and degree of disorder. Despite these theories, the precise relation between structural disorder and band-tail shape remains unclear.

The effect of band-tails is unique for the disordered phase and the influence of localized states is apparent in electrical transport, doping, recombination and other phenomena.

2.2.2 Deep Defects

In a crystal any departure from the perfect crystalline lattice is a defect, this definition then needs to be reviewed in the case of μc-Si:H. As shown in section 2.1 the particular structure of μc-Si:H is determined by (i) a lack of long range translation symmetry in the amorphous phase, (ii) a high density of twins and stacking faults within the columns, and (iii) grain boundaries. Structural defects, as defined in crystalline semiconductors, are therefore inherent parts of the system and it is not very helpful to think of it as a collection of only defects. In the context of this work it is more useful to define a defect as a deviation from the fourfold bonding configuration. This kind of defect will form for example at the grain boundaries, where the ordered lattice of the crystalline grains abruptly ends. On the other hand, Phillips has shown that for a disordered tetrahedral bonded semiconductor it is impossible to construct a ”continuous random network” (CRN) without extremely large internal stress. Broken or unsaturated bonds will therefore be formed to release the internal stress. These defects form states with an energy position between the bonding and anti-bonding states, roughly speaking in the middle of the band gap (see Fig. 2.2). In hydrogenated silicon, however, most of the broken bonds are saturated by hydrogen.

Defect Relaxation and Correlation Energy

In the case of the silicon dangling bond, the defect can exhibit three charge states. Besides the neutral D^0, where the defect is singly occupied, there are a positively charged D^+ and a negatively charged configuration D^-, where the dangling bond is occupied with zero or two electrons, respectively (see left panel of Fig. 2.2). The energy position within the band gap depends on the charge state of the dangling bond defect. Starting from a singly occupied defect (D^0), the adjoining of a second electron influences the total energy of the defects in a way, that

1. due to Coulomb interaction the two electrons repel each other splitting the energy level of the D^0 and the D^- state by the correlation energy $U_{corr} = e^2/4\pi\varepsilon\varepsilon_0 r$, where r is the effective separation of the two electrons and thus roughly the localization length of the defect wave function [65];

2. if the network around a defect is able to readjust around a negatively charged defect, this may cause a change in the bonding and lowers the energy by an amount of U_{relax}.

The effective correlation energy U_{eff} is a combination of both the Coulomb U_{corr} and the relaxation energy U_{relax},

$$U_{eff} = \frac{e^2}{4\pi\varepsilon\varepsilon_0 r} - U_{relax} \tag{2.1}$$

If the relaxation energy U_{relax} exceeds the correlation energy U_{corr} (negative U_{eff}), the energy level of the doubly occupied state D^- is smaller than the one of the neutral state D^0. Thus in an equilibrium state only D^+ and D^- defects and no singly occupied states are observed. This behavior can be found in the defect structure of e.g. chalcogenide glasses [83].

In μc-Si:H, there is a lot of experimental evidence that dangling bond states possess a positive effective correlation energy U_{eff}. In this case the level of the neutral defect D^0 lies below the one occupied with two electrons D^-, as shown in Fig. 2.2. Thus, unlike the case of the negative U_{eff}, the defect can exist in the neutral state that, due to the existence of an unpaired electron, acts as a paramagnetic center and can therefore be detected by electron spin resonance (ESR).

Paramagnetic States in μc-Si:H

The particular structure of μc-Si:H offers a number of sites where dangling bond defects can be located: the crystalline regions, the grain boundaries, the amorphous phase or due to the presence of impurity atoms like oxygen. This is the reason why, in contrast to a-Si:H, the structure of paramagnetic defects is not yet

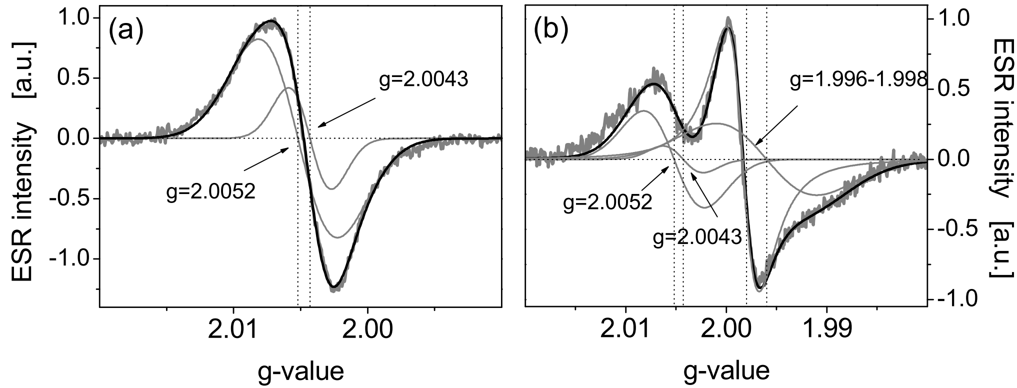

Figure 2.3: *Typical ESR-Spectra of (a) undoped μc-Si:H with contributions at g=2.0043 and g=2.0052 and (b) n-doped material with an additional contribution at g=1.998. Both spectra were taken from material investigated in this work.*

well understood. Besides the unknown microscopic location, there are also uncertainties regarding the energy positions of defects within the gap, which have been taken into account in the schematic DOS of μc-Si:H shown in the right panel of Fig. 2.2. For intrinsic μc-Si:H, the most important paramagnetic defect is the Si dangling bond (DB). An ESR spectrum of high quality intrinsic material shows an asymmetric line shape with contributions at g=2.0043 and g=2.0052. A typical spectra taken of undoped μc-Si:H material is shown in Fig. 2.3 (a). The origin of these two contributions is still controversially discussed. While it has been suggested by several authors that the anisotropy arises from two independent dangling bond states in different microscopic environments [21, 33, 35, 34, 36, 32], Kondo et al., on the other hand, assigned the two components contributing to the ESR signal to an axial symmetric g-tensor of P_b-like[1] defects located on $< 111 >$ oriented grain surfaces with components of $g_{||} = 2.0022$ and $g_{\perp} = 2.0078$ [31]. A more recent publication from de Lima et al. [84] also suggested the signal arising from an axial-symmetric center, but extracted g-values of $g_{||} = 2.0096$ and $g_{\perp} = 2.0031$, relating the signal with defects in the crystalline phase.

As microcrystalline silicon can consist of a considerable amount of amorphous phase, also dangling bond defects located in the a-Si:H fraction may contribute to the ESR signal. The DB defect found in a-Si:H has a characteristic g-value of g=2.0055 and a typical peak to peak line width of $\Delta H_{pp} = 10$ G in X-band[2] [85].

Another aspect of the increasing amorphous phase is the Staebler-Wronski-Effect (SWE) [7]. The SWE describes the light induced breaking of weak Si-Si bonds in the silicon network which leads to the creation of additional dangling

[1] P_b centers are silicon dangling bonds at the Si/SiO_2-interface of oxidized silicon wafers.
[2] For details of the notation see section 3.1.2

bond defects [86]. For highly crystalline μc-Si:H, it has been shown that it does not suffer from the SWE [19]. However, due to the presence of amorphous phase, this material might also be susceptible to light-induced metastable effects, which in fact was recently confirmed by Klein [87].

For n-type doped and also for illuminated intrinsic μc-Si:H samples, another resonance with a g-value of g=1.996-1.998 can be observed (Fig. 2.3 (b)). Since the intensity of this signal is correlated with the dark conductivity σ_D at 300 K and the g-value is close to the one of free electrons in crystalline silicon, this signal was first attributed to electrons in the conduction band [27, 29]. The resonance has therefore been referred to as the conduction electron (CE) resonance. Later on, this signal has also been attributed to localized states in the conduction bandtail [88, 35, 38, 39, 72].

Substitutional Doping

Controlled incorporations of impurities are typically used to provide additional free charge carriers. Typical donors and acceptors used to dope silicon are phosphorus and boron, respectively. In crystalline silicon (c-Si), the inclusion of dopants immediately lead to a shift of the Fermi level E_F up to an energy position, located between the energy level of the dopant and the band edge, even for very low doping concentrations. In contrast to crystalline silicon, the high concentration of intrinsic defects has a major influence on the free carrier concentration achieved from doping. Additional incorporation of e.g. donors will be compensated by the defects as they act as acceptors by creating D^- states, accumulating the charge carriers. This is the reason why deep defect states within the band gap first have to be compensated before the Fermi level can shift to the conduction band edge.

For amorphous silicon another complication prevents that high doping densities can be achieved. The doping induces deep states in the gap preventing a shift of the Fermi level [89, 90]. Different, independent experiments have shown that the total defect density increases with the square root of the doping concentration [65].

2.3 Charge Carrier Transport

In crystalline silicon, the charge carrier transport takes place in the extended states of the band and can be described using effective mass theory [91]. In μc-Si:H, on the other hand, the presence of localized states within the bandgap has a major

influence on the transport properties and has to be considered in models used to explain transport features. The existence of band-tail states and deep defects may open new transport paths or they might act as traps for charge carriers or form barriers.

In the past, various models have been proposed adopting and combining models successfully used to describe transport data from either poly-crystalline or pure amorphous material. As μc-Si:H consists of small crystals separated by grain boundaries, first attempts to explain the transport behavior were done adopting the model of "grain boundary trapping" developed for polycrystalline silicon by Seto [41] and further extended by Baccarani et al. [92]. On the other hand, the existence of band-tail states suggests that transport might take place by direct tunneling between localized states (hopping) or by trap-limited band motion (multiple trapping). In the following section a phenomenological description of these ideas and their consequences will be given.

2.3.1 Barrier Limited Transport

The model of barrier limited transport is based on the ideas of Seto [41] and got a further improvement by Baccarani [92] (see also [93]). It is successfully used to describe the transport behavior of poly-crystalline silicon. As microcrystalline silicon consists of crystallites separated by grain boundaries, the model proposes that the transport properties are mainly determined by defect states located at the grain boundaries. Charge carriers can be trapped and ionize these states leading to potential barriers. Charge carriers overcome these barriers by thermionic emission. Temperature dependent measurements done by Spear et al. [94] and Willeke [95] seemed to prove this model showing the characteristic temperature activated mobility expected for barrier limited transport, but have only been performed in a small temperature range. On the other hand, conductivity measurements over a wide range of temperatures showed that μc-Si:H does not exhibit a single activated transport behavior [44]. Lately this model has been further refined by including tunneling as a process to overcome the barriers [42] in order to explain Hall mobilities of n-type μc-Si:H. A detailed discussion of barrier-controlled transport in microcrystalline semiconductors can be found e.g. in Refs. [42, 96].

2.3.2 Dispersive Transport in Disordered Semiconductors

On the other hand, the existence of a broad tail of states extending into the gap (see section 2.2.1 for details), suggests that these states play an important role in the transport mechanism. As discussed above, band-tail states are a result of structural disorder. A typical transport feature found in disordered materials is that of

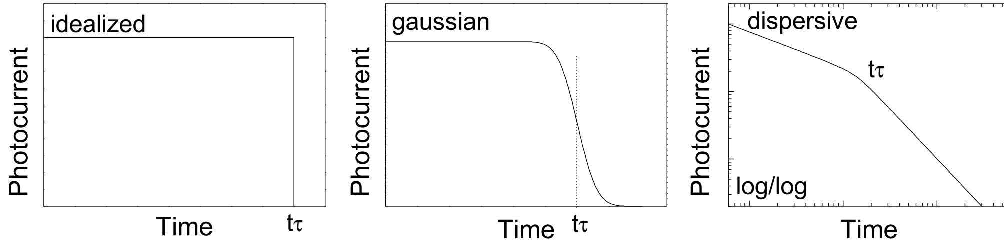

Figure 2.4: *Current pulse shapes obtained in a time-of-flight experiment. The different shapes are a result of different transport mechanism leading to different degrees of dispersion as described in the text.*

dispersive transport. In Fig. 2.4 transient photocurrents are shown. Experimentally, these currents can be measured by e.g. time-of-flight experiments (TOF), described in section 3.1.4.

In a TOF experiment, the material of interest is usually packed between two contacts and the time required for a charge carrier packed to drift from one side of the sample to the other is measured. The left panel of Fig. 2.4 shows an idealized current following the generation of charge carriers. It describes a sheet of charge, photoinjected on the front side of the sample, moving across the specimen with a constant velocity. The current breaks down at the transit time t_τ where the charge carriers reach the back contact. In practice, however, the initially discrete packet of charge carriers will broaden as it drifts across the specimen (middle panel of Fig. 2.4). The dispersion w is a consequence of statistical variations in scattering processes and carrier diffusion which is connected to the drift mobility through the Einstein relation ($D = \frac{kT}{e}\mu_d$). When the first carriers arrive at the back contact, the current starts to drop, the width of the current decay is a measure of the dispersion at that time. In this case the transit time is defined as that time at which the mean position of the charge carrier packet traverses the back electrode. This is equal to the time, where half the charge has been collected. Because of the shape of the dispersion it is referred to as Gaussian transport in the literature.

While transit pulses of the form shown above are observed in many crystalline and some amorphous solids, in some cases they differ significantly. A typical current transient shape for such a case is shown in the right panel of Fig. 2.4 (note the log-log scale). Quite surprisingly, the current appears to decrease over the whole time range of the measurement. Even at times prior to the transit time t_τ the current does not show a constant value as observed for Gaussian transport. Perhaps the most outstanding feature is that as a function of time the current decays approximately linearly on a logarithmic scale, indicating a power-law behavior. The two linear regimes are separated by a time t_τ and show the following time distribution

function

$$I(t) \propto \begin{cases} t^{-(1-\alpha_1)} & t < t_\tau \\ t^{-(1+\alpha_2)} & t > t_\tau. \end{cases} \tag{2.2}$$

The dispersion parameter $\alpha_{1,2}$ is determined by the disorder of the material [97]. Note that Eq. 2.2 has no characteristic long time cut-off, in fact, even at times greater than $2t_\tau$ the magnitude of the current suggests that still a significant number of charge carriers remains within the specimen. Such a high degree of dispersion occurs when during transport the average charge carrier experiences a single localization event with a time that is comparable with the mean transit time defined by the applied voltage and the sample thickness [98]. A second phenomenon observed is the universality of the transient current pulse shape. Transient currents measured for a given sample at different applied fields exhibit the same degree of relative dispersion. This behavior also extends to variations in the sample thickness.

To account for the high degree of dispersion, two mechanism have been proposed, namely hopping and trap-limited band transport.

Hopping

In a hopping system, developed by Scher and Montroll [99], the transport is based on hopping and tunneling of the charge carriers between states. The probability for a transition varies with the separation R of two sites as $\exp(-2R/R_0)$, where R_0 is the localization radius of the state (equal to the effective Bohr radius for localized carriers) [68]. If the mean intersite distance $\bar{R}$ is large compared to R_0, one will observe a wide spread of the probabilities to escape from a state and the broadening of the charge carrier packet is highly pronounced. The dispersion arises from the random distribution of the site separation. The immobilized carriers are trapped in centers more isolated from their neighbors than the average distance. With increasing time, the drifting carriers will be more and more accumulated in more isolated sites with longer release time constants. This results in the observed continuously decaying current even for very long times.

Hopping in an exponential band-tail has been applied to describe the transport behavior of μc-Si:H in the low temperature region [46, 47] as well as the behavior found at elevated temperatures [46, 48].

Multiple Trapping in Band-Tails

A number of studies in 1977 showed that dispersive transport can also arise from trap-limited band transport [100, 101, 98, 102, 103]. In a multiple trapping model, charge transport only takes place in the extended states of the band. Charge carriers trapped in localized states are immobile and must first be thermally excited

above the mobility edge to contribute to transport. It has been shown by Schmidlin [98] that for anomalous dispersion to be generated, the concentration of the localized states must accomplish the following two criteria. First, a charge carrier is likely to be trapped in a localized state at least once during the transit and second, the release time of a carrier trapped in a localized state must be comparable to the transit time t_τ [98]. As has been discussed above (see section 2.2.1), the band-tails in μc-Si:H are expected to decrease exponentially towards the gap. Provided that the localized states in the vicinity of the mobility edge all to have the same origin, e.g. potential fluctuations, the energy dependence of the capture cross section is probably weak [104], so that each localized state has the same probability to capture a charge carrier. However, the exponential dependence of the thermal re-emission leads to a broad distribution of release times. The dispersion arises from the energy distribution of states and since thermal excitation is involved, both the mobility and the dispersion strongly depend on temperature.